View metadata, citation and similar papers at core.ac.uk
brought to you by CORE
provided by CiteSeerX

PERGAMON

Acta mater. 48 (2000) 2689–2701

Acta MATERIALIA

www.elsevier.com/locate/actamat

THE DEVELOPMENT OF SPATIAL CORRELATIONS DURING OSTWALD RIPENING: A TEST OF THEORY

V. A. SNYDER, J. ALKEMPER and P. W. VOORHEES†

Robert R. McCormick Sch. Eng. & App. Sci., Department for Materials Science and Engineering, Northwestern University, 2225 N. Campus Dr., Evanston, IL 60208-3108, USA

(Received 23 December 1999; accepted 23 January 2000)

Abstract—The coarsening of solid-Sn particles in a Pb–Sn liquid was studied under microgravity conditions. Spatial correlation functions were measured on plane sections in a low-volume fraction system undergoing Ostwald ripening. The correlation functions changed with time in a way that indicated that the microstructure initially consisted of clusters of particles and evolved into one which was more dispersed. The model by Akaiwa and Voorhees (AV) was used to study the effect of spatial correlations on the ripening process. We found that the initially highly correlated structure had no observable effect on the evolution of particle size distributions, but did have an effect on the coarsening rate of the system. Specifically, we determined that a structure consisting of clusters of particles coarsened faster than a system with a random, spatial arrangement of non-overlapping particles. We also found that the approach of the microstructure towards the steady-state regime could be monitored more sensitively using spatial correlations rather than using particle size distributions. The spatial correlations and the particle size distributions measured from the experiment agreed well with those calculated from the AV simulations using the initial experimental correlations and size distribution. © *2000 Acta Metallurgica Inc. Published by Elsevier Science Ltd. All rights reserved.*

Keywords: Phase transformations; Nucleation; Growth; Theory and modeling (kinetics, transport, diffusion)

1. INTRODUCTION

Ostwald ripening, or particle coarsening, is a process in which a system lowers its energy by reducing its interfacial area. Coarsening occurs by the dissolution of small particles and the growth of large particles. This results in an increase in the average particle size over time, and a concomitant decrease in the number of particles in a system.

The classical description of coarsening was developed by Lifshitz and Slyozov [1] and Wagner [2] (LSW). They determined the evolution of the microstructure for a system of infinitely separated spherical particles, or a zero volume fraction of coarsening phase. LSW found that in the long-time limit, the system approaches a self-similar regime. In this regime, the particle size distribution (PSD) becomes time invariant when scaled by the time-dependent average particle radius. The average particle radius, $\bar{R}(t)$ increases with time, t, as

$$\bar{R}^3(t) - \bar{R}^3(0) = Kt \tag{1}$$

where K is the coarsening rate constant for an isothermal solid–liquid system given by [3]:

$$K = K_{\mathrm{LSW}} = \frac{8}{9}\frac{T_0 \Gamma D}{M_{\mathrm{L}}(C_{\mathrm{S}} - C_{\mathrm{L}})}. \tag{2}$$

T_0 is the coarsening temperature, Γ is the capillary length of the matrix phase, D is the diffusion coefficient of the solute in the liquid, M_{L} is the slope of the liquidus curve at T_0, and C_{S} and C_{L} are the compositions of the solid and liquid at a planar solid–liquid interface at T_0. K_{LSW}, thus, is a function only of various material parameters.

Many theories have since been developed to account for a finite volume fraction of particles and thus for overlapping diffusion fields between particles [4–12]. The theories differ in their methods of determining a statistically averaged growth rate for a particle of a given size. Most theories are limited to low-volume fractions of particles (≤ 0.3), since above this volume fraction the assumption of spherical non-touching particles is poor. Exceptions are effective medium theories that make predictions at much higher volume fractions [8, 9]. All of the theories have found that a finite volume fraction of particles does not alter the temporal exponent of

† To whom all correspondence should be addressed.

1359-6454/00/$20.00 © 2000 Acta Metallurgica Inc. Published by Elsevier Science Ltd. All rights reserved.
PII: S1359-6454(00)00036-7

the average particle radius of 1/3. A non-zero volume fraction, however, does alter the coarsening rate such that K is a function of the volume fraction of coarsening phase, ϕ, as given by,

$$K = K(\phi) = K_{\mathrm{LSW}} f(\phi) \tag{3}$$

with $f(\phi)$ being a system-independent function of the volume fraction. The theories recover the LSW results at zero volume fraction [$f(0) = 1$]. Despite this general agreement, the predictions of $f(\phi)$ and the form of the PSDs differ from theory to theory.

Many theories assume that the particles are randomly distributed in the matrix [6–12]. However, interparticle spatial correlations may play a role in the coarsening process [4, 10–12]. Akaiwa and Voorhees studied the evolution of the spatial correlations in transient as well as the steady-state coarsening regime, using both monopole and dipole approximations for the diffusion field in their simulations. In their work, two different initial spatial arrangements of particles were found to coarsen to a unique time-invariant arrangement when properly scaled. These steady-state correlation functions were different than those of a random distribution of particles. They also found that the evolution of the spatial arrangement of particles had only a small effect on the coarsening rate of the system. Size–size correlations were also measured, and they found that the density of small particles near large particles was less than that of a random spatial distribution. Beenakker [10] employed a much smaller system than Akaiwa and Voorhees in a monopole simulation, but was able to calculate moments of the pair correlation function. He found that the spatial correlations present in the system were not those of a random non-overlapping distribution of particles. Tokuyama and Kawasaki [11] calculated the structure function during steady-state coarsening. Since the structure function depends on both the PSD and the spatial correlation function, it is not possible to determine the predicted spatial arrangement of particles. Thus, this result can only be tested using X-ray or neutron scattering experiments. Marder [12] developed a theory which takes into account spatial correlations present in a coarsening system. However, the correlations measured in his work are different than those found by Beenakker and the rate constant determined in his work is much larger than any other theoretical prediction with one exception [13]. Spatial correlations that develop during coarsening have also been studied in two-dimensional systems. Akaiwa and Meiron [14] used numerical simulations with monopole and dipole approximations to describe coarsening with two different initial spatial distributions of particles. They also found time invariant spatial correlation functions in the steady-state regime, despite the different initial conditions. In addition, they found excellent agreement with two-dimensional Ostwald ripening experiments performed by Krichevsky and Stavans [15].

Many experiments have found a temporal exponent of nearly 1/3 for the average particle size during coarsening [3, 16, 17]. However, experimentally measured PSDs are broader than steady-state predictions made by theory [18]. Comparatively little work has been done experimentally to measure spatial correlations during coarsening due to the large amount of data necessary for such measurements. Small-angle neutron scattering experiments on Al–Li alloys show the presence of correlations between δ' precipitates during ripening; see for example [19]. However, these were measurements of the structure function not of the spatial correlation function. Spatial correlations have been measured during liquid phase sintering in systems with high-volume fractions of solid [20]. Unfortunately, the high-volume fractions of the coarsening phase employed in these experiments preclude a comparison to the aforementioned low-volume fraction theories. In addition, the correlations are likely influenced by the skeletal structure that forms in these systems. Correlations have been measured in a system of particles coarsening by aggregation [21], and in two dimensions [15]. The correlations of a system undergoing coarsening in three dimensions, where the volume fraction is sufficiently low that a direct comparison between theory and experiment is possible, have never been measured.

In the present work, we have measured correlations that are present in a low-volume fraction system in which the particles coarsen solely by Ostwald ripening. We measured the correlations in real space, not using X-ray or neutron scattering experiments, which allows us to determine the spatial correlations independent of the PSD. Both the coarsening experiments and the model which is tested are in a system that is three-dimensional. However, the comparison of theory and experiment was made using planar sections through the three-dimensional microstructures, thus avoiding difficulties in converting plane section measurements to three dimensions. The measurements were made on samples containing 10% and 20% coarsening phase, for which no skeletal structure is present. Since the samples were coarsened in a microgravity environment, there was no particle sedimentation caused by a density difference between the phases. In addition, we used an ideal two-phase mixture which satisfies all of the assumptions of theory. Thus, it is possible to make an unambiguous comparison between theory and experiment.

In addition to examining the spatial correlations that develop during coarsening both theoretically and experimentally, we have reanalyzed data presented earlier on the coarsening kinetics and PSDs at a volume fraction of 0.1 coarsening phase [18]. It was shown that these measured distributions were broader than the steady-state theoretical predic-

tions, and most importantly, that they were slowly evolving in time. The rate constant was also higher than those predicted by steady-state theories. In order to address the apparent evolution of the PSD, two different theoretical models [4, 22] were employed to study transient coarsening. We found excellent agreement of the evolution of the PSDs between the experiment and both models. The initial microstructure used in these transient simulations employed a size distribution that was the same as that measured at an early coarsening time. However, we did not account for the highly correlated microstructure, consisting essentially of clusters of particles, which was present at early coarsening times. We define a cluster of particles as being a set of non-overlapping particles that are spatially close together. A more accurate model of the transient coarsening process is presented here, as we have now included the effect of the initially strong spatial correlations on the coarsening process. Results at a volume fraction of 0.2 are also shown for the first time.

First, the experimental results from the coarsening in solid–liquid mixtures experiment (CSLM) are presented. These results motivate the inclusion of spatial correlations in the Akaiwa and Voorhees simulations, as the experiments at early times reveal a microstructure containing clusters of particles. A direct comparison of the evolution of the PSDs and the spatial correlation functions is made between our new model, which includes the effects of spatial correlations, and the experiment. We conclude with a discussion and summary.

2. EXPERIMENT

2.1. Experiment procedure

A two-phase mixture consisting of solid-Sn particles in a Pb–Sn liquid has been identified as an ideal system to study Ostwald ripening: the coarsening rate is rapid such that experiments can be performed in a timely manner, the interfacial energy is nearly isotropic giving rise to spherical particles in the matrix, and the thermophysical parameters of the system have been measured [23].

Samples of Pb–Sn were prepared using the method previously employed by Hardy and Voorhees [3]. To prevent particle sedimentation, samples were processed in microgravity in the Microgravity Science Laboratory aboard Space Shuttle Columbia during the space-flight missions STS-83 and STS-94. Samples were retrieved from the shuttle, sectioned, etched, and photographed. Several images were then taken from each section and montaged together to form images of entire sample cross-sections. PSDs and spatial correlation functions were measured on these plane sections (PS). The montaging minimizes edge effects which could influence spatial measurements of the microstructure. The results shown here are for the 10% and 20% volume fraction samples. Between 2000 and 10,000 particles were used for each measurement at a given volume fraction and coarsening time. The shortest coarsening time analyzed was 550 s, as the furnace had not reached a thermal equilibrium before this time.

The radial distribution function measured on a plane section (RDF) is used to quantify the spatial arrangement of features in a microstructure. The plane section RDF is defined as the ratio of the number of particles per area whose centers lie within a circular shell of radius x and thickness $\mathrm{d}x$ surrounding a particle, to the number of particles per area of the entire system,

$$\mathrm{RDF_{PS}}(x) = \frac{N_\mathrm{A} \text{ in a circular shell of radius } x \text{ to } x + \mathrm{d}x}{\bar{N}_\mathrm{A}} \tag{4}$$

where N_A is the number of particles per area and $\bar{N}_\mathrm{A}$ is the overall particle density. For any spatial distribution of particles, $\mathrm{RDF_{PS}} \to 1$ as $x \to \infty$.

2.2. Experimental results

Microstructures obtained from four of the nine samples with a volume fraction, $\phi = 0.1$, are given in Fig. 1 for coarsening times of 880, 5810, 14,400 and 36,600 s. The Sn particles are shown in white and the Pb–Sn liquid matrix is shown in black. These microstructures are scaled by the plane section average radius at each time, and thus all of the samples appear to have similar particle sizes. The microstructures in Figs 1(a) and (b) show a clustering of particles, which is a remnant of the sample manufacturing procedure. The clustering effect is less evident in the microstructure in Fig. 1(c), and has vanished by the final coarsening time of 36,600 s. If the steady-state coarsening regime had been reached, these microstructures would appear time-invariant. This is clearly not the case.

The clustering can be quantified by measuring the spatial correlations in the system. RDFs for the 10% volume fraction samples are shown at several coarsening times in Fig. 2(a). At the 880 s coarsening time, the RDF has a large peak at $x/\bar{R}_\mathrm{PS} \approx 2.2$, indicating that the particles are indeed clustered as Fig. 1(a) shows. Over time, the peak decreases and shifts to the right, indicating that an exclusion zone of increasing size is developing around each particle, in agreement with Figs 1(b)–(d). The RDFs for the two longest coarsening times analyzed with respect to spatial correlations, 9510 s (not shown) and 14,400 s, are nearly identical, with a much smaller peak at $x/\bar{R}_\mathrm{PS} \approx 3.5$. This could be an indication that the steady-state coarsening regime has been reached, but it could also be due to a slower evolution of the microstructure at long times.

Also shown in Fig. 2(a) is the predicted steady-

state RDF_{PS} given by the AV theory for $\phi = 0.1$. The predicted steady-state correlations have a much larger exclusion zone surrounding the particles than those measured in the experiment. During coarsening, the microstructure becomes much more dispersed, but never reaches the steady-state prediction, even after 14,400 s. Interestingly, the RDF_{PS} measured at a coarsening time of 14,400 s is similar to that of a random non-overlapping set of particles with the same PSD. The sample coarsened for 36,600 s had a large shrinkage pore that disturbed the spatial arrangement of particles; therefore, a meaningful RDF could not be measured for this coarsening time.

The evolution of the RDF at $\phi = 0.2$ is also shown in Fig. 2(b). The evolution of these correlations is less drastic than the evolution at $\phi = 0.1$, but shows the same trend. The peak in the RDF decreases with time and the curve shifts slightly towards the right. At 14,400 s, however, the RDF for $\phi = 0.2$ has a larger peak than the RDF for $\phi = 0.1$. The small change in the RDF may be due to the smaller particle-free volume at $\phi = 0.2$ than at $\phi = 0.1$.

PSDs were also measured during the experiment [18] and are shown in the next section in direct comparison with results from the simulations. Although it was not possible to measure the RDF

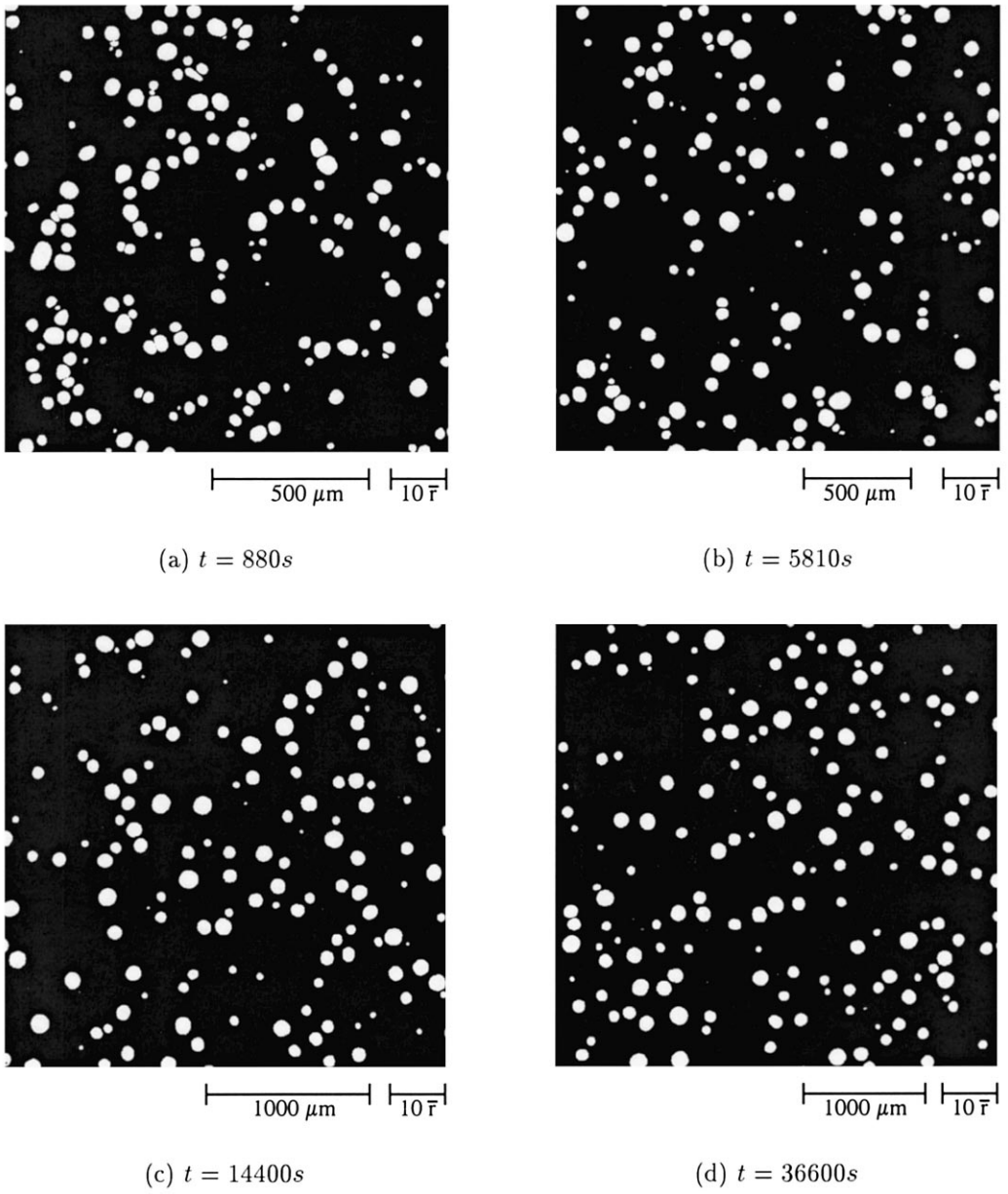

Fig. 1. Microstructures of the solid–liquid mixture.

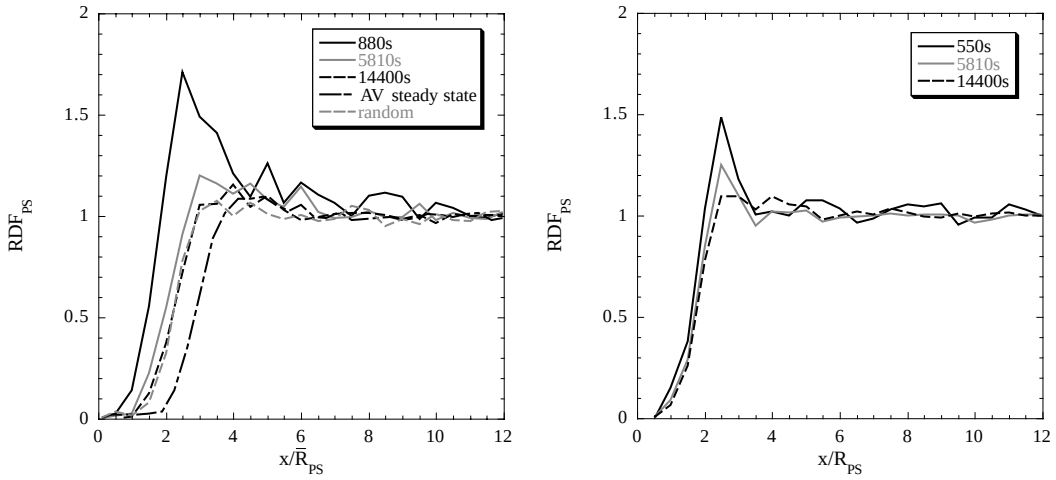

(a) $\phi = 0.1$ (b) $\phi = 0.2$

Fig. 2. The temporal evolution of the PS spatial correlation functions for volume fractions of 0.1 and 0.2.

at 36,600 s for the sample with $\phi = 0.1$ due to the large pore that formed upon solidification, this pore should not have affected the PSD. We thus can safely compare theory and experiment at t = 36,000 s.

3. SIMULATIONS

3.1. Simulation procedures

In order to study the evolution of the microstructure observed in the coarsening experiments, numerical simulations based on a theory developed by Akaiwa and Voorhees (AV) [4] are used. This theory is employed for two reasons: (1) it appears that the experiments might not be at steady state, thus a theory which is valid in the transient regime is required; and (2) the AV theory makes no *a priori* assumptions on the spatial correlations present in the system. In this theory, numerical simulations are employed to model a discrete set of particles undergoing coarsening. Individual particle growth rates are determined by numerically calculating the diffusion field surrounding each particle. By using this method, multi-body diffusional interactions can be taken into account without any assumption on the spatial correlations present in the system. In particular, any given spatial distribution of non-overlapping particles with any PSD can be employed as initial conditions in this simulation.

Before comparing theory and experiment, the effects of spatial correlations on the coarsening process were investigated. In order to study how the spatial correlations influenced the coarsening rate and the evolution of the microstructure, simulations were performed with both clustered and random initial spatial distributions. A microstructure consisting of clusters of particles was investigated, since it is the initial microstructure found in the experiments.

A comparison was also made between the CSLM experiment and the AV theory. Specifically, the PSDs and the RDFs as measured from the experiment at different coarsening times are directly compared to those calculated from the numerical simulations. The simulations used spherical particles at volume fractions of either 0.1 or 0.2 coarsening phase. The timescale of the simulations is set by the initial average radius and the value of K_{LSW} for the system. To match the simulations with the experiments, we used an initial average PS radius of 17.77 μm for $\phi = 0.1$ and 15.82 μm for $\phi = 0.2$, as found in the 880 s and 550 s experiments, respectively, and $K_{LSW} = 1.6$ μm^3/s for simulations with $\phi = 0.1$ and $K_{LSW} = 1.7$ μm^3/2 for $\phi = 0.2$. The method by which this K_{LSW} is obtained will be discussed later.

Two sets of simulations were performed with a volume fraction of 0.1. Each set consisted of two simulations. Each simulation employed a unique set of approximately 50,000 particles at the beginning of the simulation. The measurements from the individual simulations within each set were averaged to improve statistics. Both sets of simulations used an initial PSD that matched the PSD_{PS} found in the experiment at the coarsening time of 880 s. The initial spatial correlations for the first simulations were those of a random, non-overlapping spatial distribution of particles. The second set of simulations employed an initial spatial distribution of particles with a correlation function which matched that of the 880 s coarsening experiment. The highly clustered structure present at 550 s in the samples with $\phi = 0.1$ caused particle overlap during our simulations. Thus, we chose the less clustered struc-

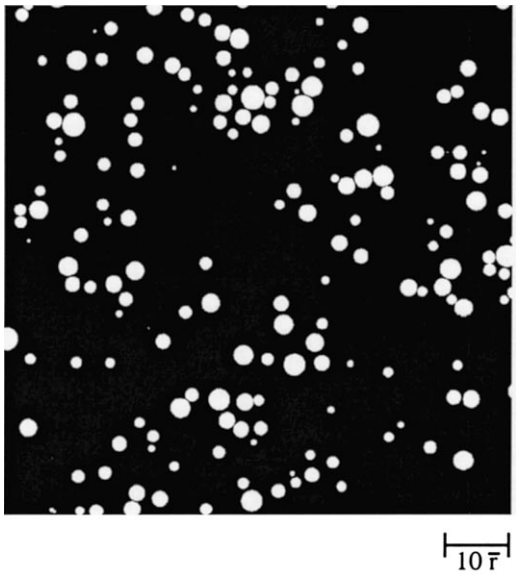

Fig. 3. The initial microstructure developed for the simulations with $\phi = 0.1$.

ture that was present at 880 s as the initial condition.

Two simulations were performed with a volume fraction of 0.2 coarsening phase. Each simulation employed 17,000 particles at the start of coarsening with a PSD and RDF that matched those found in the 550 s experiment. Simulations with initially random correlations were not run at this volume fraction.

All of the microstructures used in the simulations were developed by placing particles, which fit the three-dimensional PSD for the experimental coarsening time of 880 s (550 s for $\phi = 0.2$), randomly, but not overlapping in a simulation box. The particles for the second set of simulations were then moved from these locations to form several clusters of particles that were randomly located in space. The particles were not allowed to touch. The clustering was done until PS spatial correlation functions matched those of the 880 s experiments. During this process it was found that the number of particles per cluster is an important factor in matching the experimental and theoretical RDFs. The number of particles in a cluster affected the width of the initial large peak in the RDF and was varied until the RDF matched that of the experiment. A slice of the microstructure created for the simulations at $\phi = 0.1$ is shown in Fig. 3. The strong correlations present in this structure are apparent and the microstructure can be compared directly to the microstructure obtained from the experiments at 880 s, shown in Fig. 1(a). The main difference between these two microstructures is seen only in the circularity of the particle cross-sections.

3.2. Simulation results

The evolution of the RDFs for both the simulation using the random distribution of particles and the simulation using the experimentally measured RDF are shown in Figs 4(a) and (b). The evolution of the random structure can be characterized as the growth of an exclusion zone surrounding each of the particles. On average, the interparticle separation is larger during coarsening than for a random distribution. There is also a small peak in the RDF, which disappears early in the simulations and reappears by t = 86,000 s. The evolution of the highly correlated structure is characterized by a decrease in the height of the large peak present in the initial RDF. Thus, over time, the clustering is

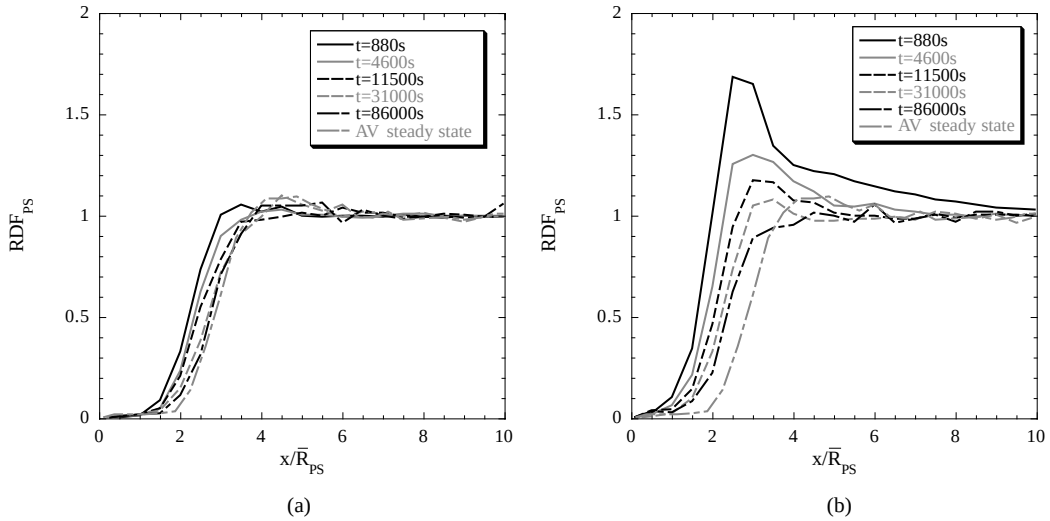

Fig. 4. The evolution of the PS spatial correlation functions for the simulations of a microstructure with (a) random correlations and (b) strong correlations.

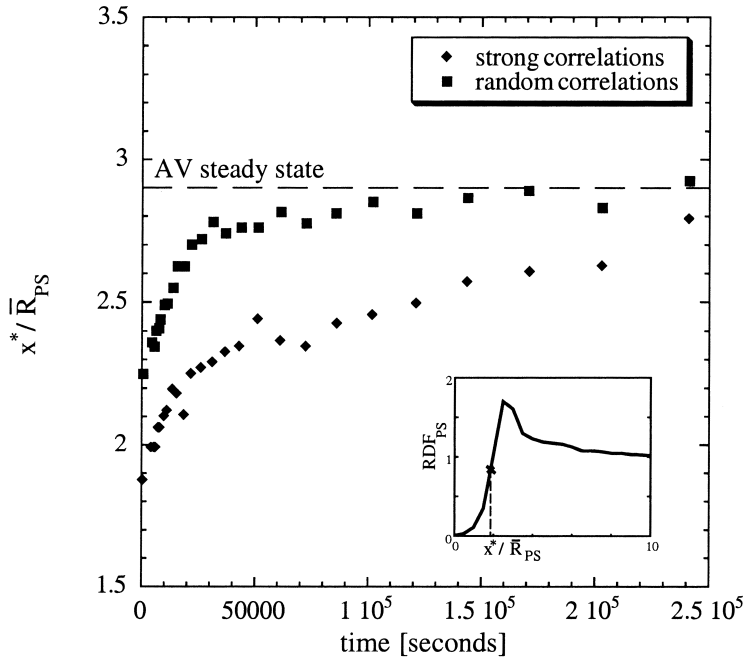

Fig. 5. The size of the exclusion zone is plotted as a function of time. The dashed line shows the AV steady-state prediction.

reduced in the microstructure, and the exclusion zone surrounding each of the particles grows. The RDF for a microstructure with random correlations lies between the RDFs shown at t = 31,000 and 86,000 s in Fig. 4(b). This shows the evolution of the clustered structure to a microstructure with random correlations and then given a sufficient amount of time will reach steady-state.

As seen in Fig. 4(b), the evolution of the RDF is manifested by a growth in the exclusion zone and a decrease in the peak height, both of which are closely related to each other. Thus, in order to

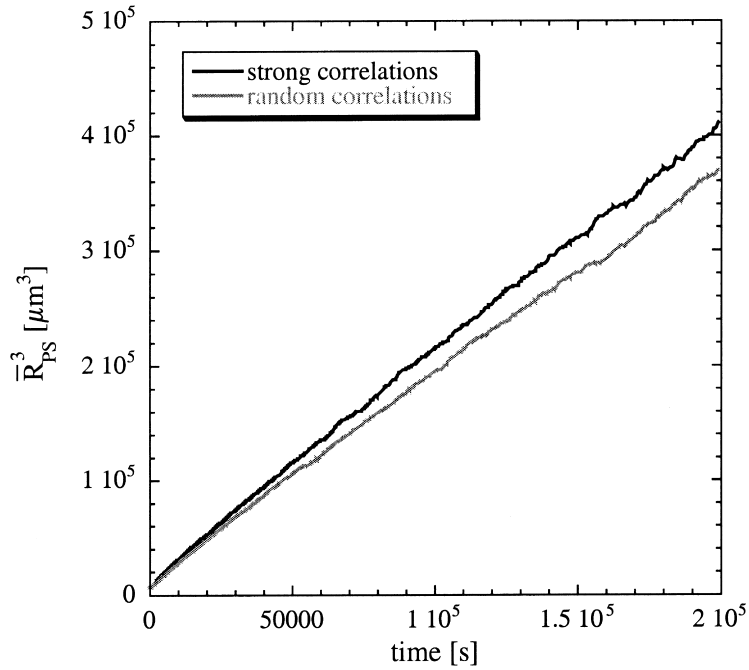

Fig. 6. Cube of the average particle size vs t for simulations with strong correlations, shown in black, and random correlations, shown in grey.

track the evolution, we have measured the size of the exclusion zone and plotted its evolution with time in Fig. 5. The exclusion zone surrounding the particles is quantified by measuring the radial distance to half the peak height, x^*; see the inset of Fig. 5. This parameter is measured for the simulations both with the strongly correlated and randomly correlated initial spatial distributions at $\phi = 0.1$.

The simulations which coarsen from a random structure have a larger exclusion zone than the simulations which coarsen from the correlated structure throughout the duration of the simulations. The growth of the exclusion zone can clearly be seen in both simulations. The growth is initially rapid and then slows as the microstructures approach steady-state. Near the end of the simulations, the limited number of particles left in the system make the correlation functions too noisy to measure the size of the exclusion zone accurately. From this figure, we clearly see that the microstructure with random correlations reaches the steady-state regime before the microstructure with the initially strong correlations, measured from the experiment.

The computed evolution of the average particle radius is shown in Fig. 6 for $\phi = 0.1$. The system with the originally clustered microstructure coarsens approximately 10% faster than a system of randomly distributed particles, as can be seen by comparing the slopes of the curves in Fig. 6.

3.3. Comparison between simulations and experiment

The evolution of the microstructure from the coarsening simulations can now be compared to

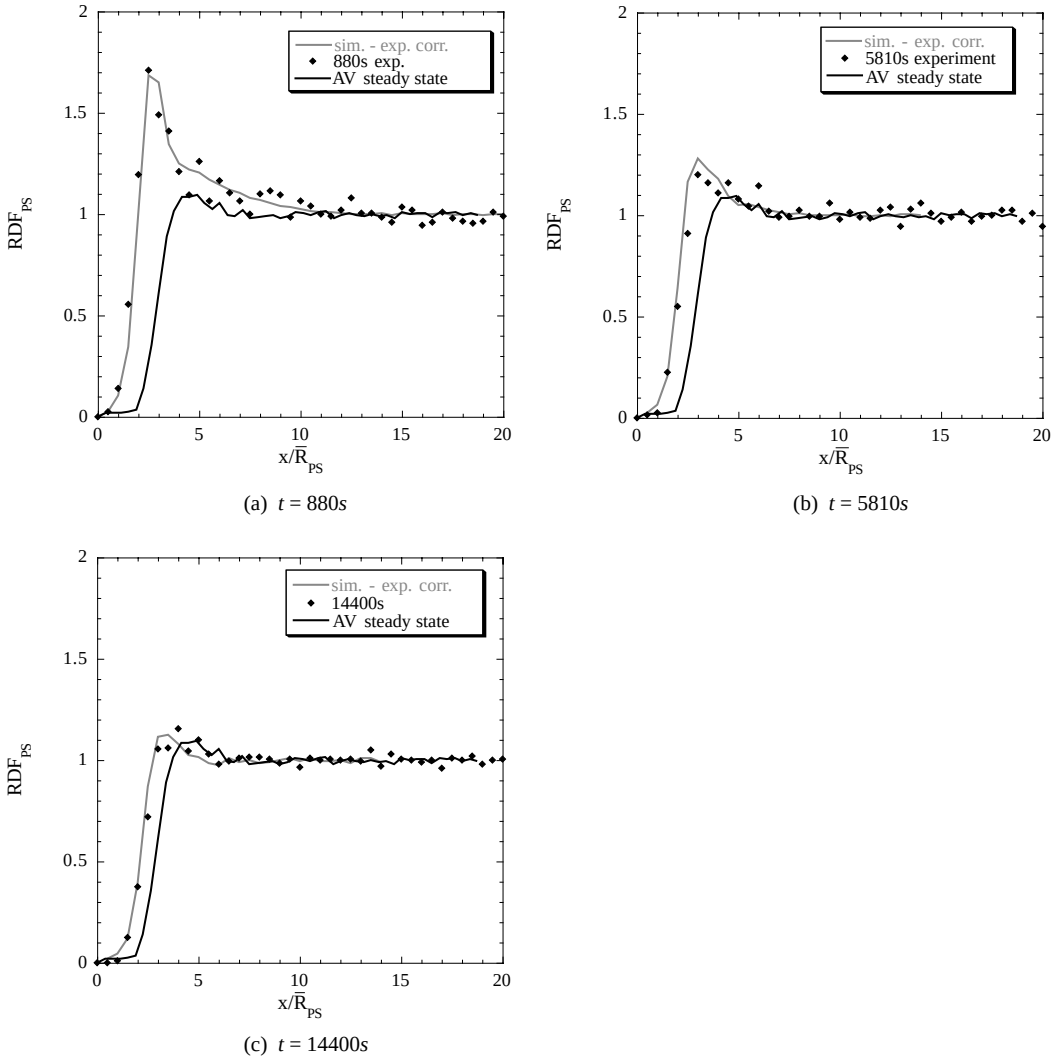

Fig. 7. The evolution of spatial correlations present in the experiment and the simulations for $\phi = 0.1$. The grey lines show simulation results and the black diamonds show results from the experiment. The AV steady-state prediction for $\phi = 0.1$ is shown in black.

that from the experiment. The spatial correlations measured for the 880 s experiment were used as an initial condition for the simulations. The evolution of the correlations for both the experiment and the simulations are shown in Fig. 7 for $\phi = 0.1$. The computed PS correlations agree very well for later times; see Figs 7(b) and (c). In particular, the experimental and theoretical correlations have similar exclusion zone widths. The simulations follow the experiment very well, and it appears that neither has reached steady state at $t = 14{,}400$ s.

The PSDs were also measured during the experiment and compared with the AV theory. The computed PSDs using an initial random distribution of particles [18] are similar to the PSDs using the experimentally measured correlations, thus it is only necessary to show the PSDs that start from a correlated structure. Thus, we found that the correlations had little or no effect on the evolution of the PSDs. The PSD used as the initial condition in the simulation is chosen to agree with the experimentally measured PSD, as shown in Fig. 8(a). As time increases, the PSD first broadens and then becomes sharper with the peak shifting to larger ρ. This behavior is seen both in the experiment and the simulations in Fig. 8. Even at the final two experiment times of 14,400 and 36,600 s, the PSDs from the simulations are close to those of the experiment. The PSDs from the experiment are slightly narrower than the simulation results, but this is due to the sensitivity of the simulations to their initial conditions. Neither the transient simulations nor the experiments have reached the steady-state prediction by the longest coarsening time.

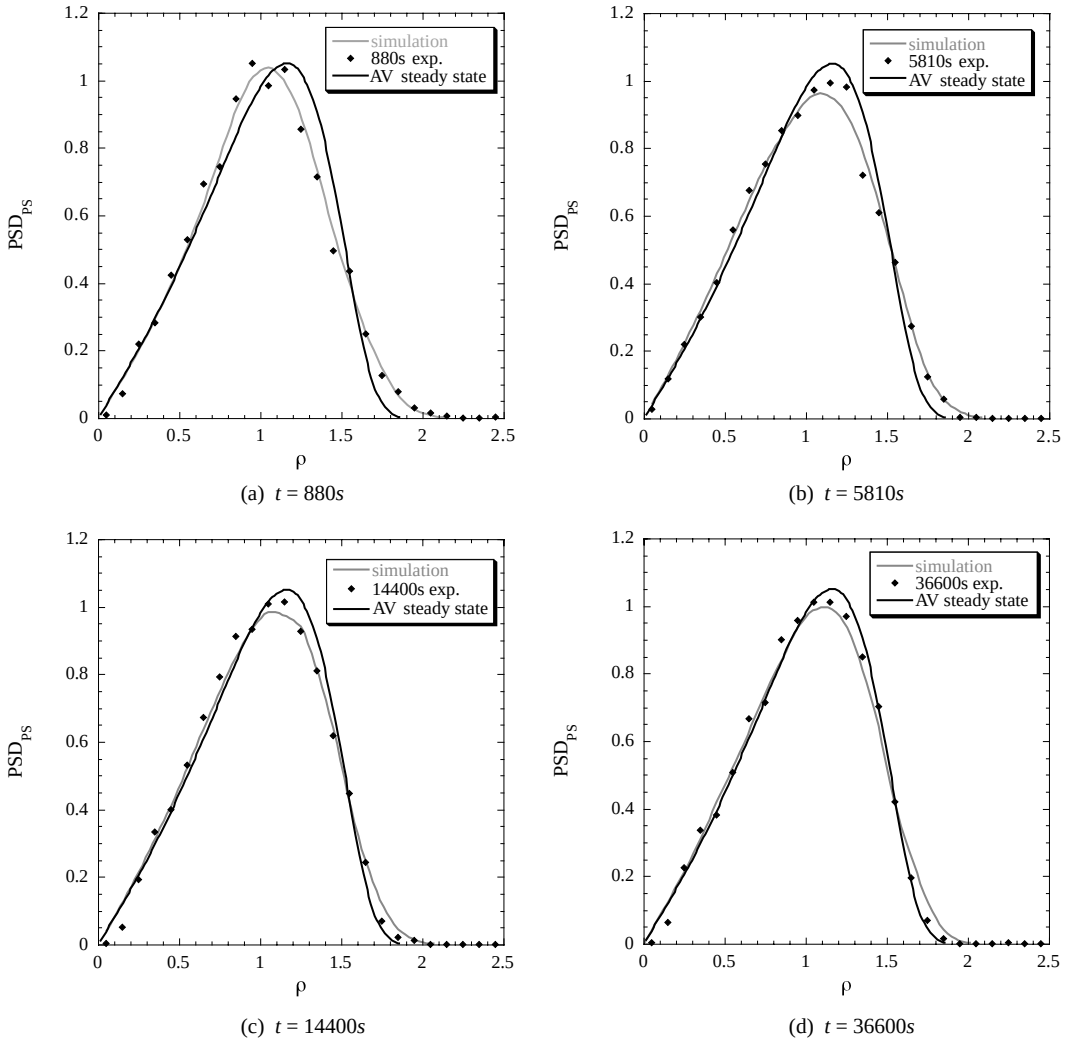

Fig. 8. The evolution of the PSDs in the experiment and the simulations for $\phi = 0.1$. The grey lines show simulation results, the diamonds show results from the experiment, and the black lines show the predictions of steady state. ($\rho = R/\bar{R}_{PS}$.)

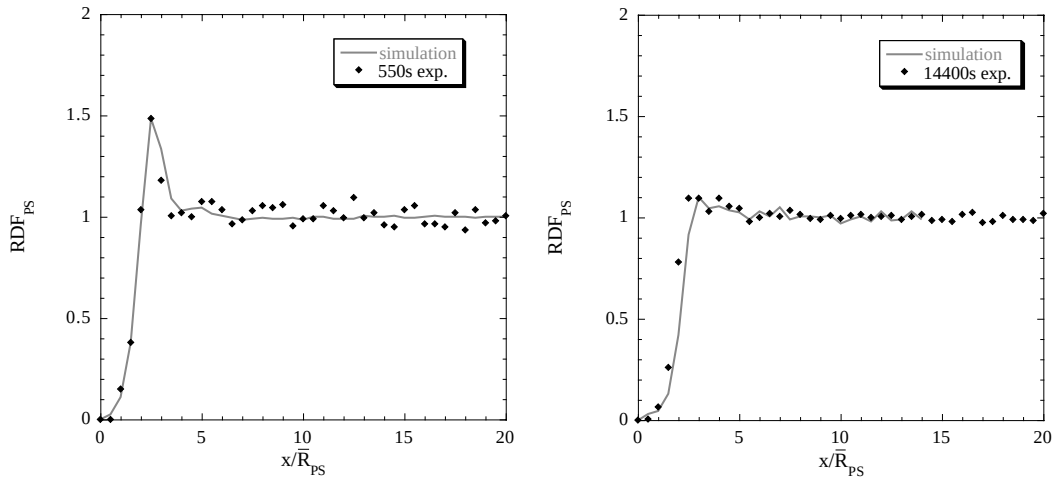

(a) $t = 550s$ (b) $t = 14400s$

Fig. 9. The evolution of the RDF in the experiment and the simulations. The solid grey lines show results from the simulations, the diamonds show results from the experiment at $\phi = 0.2$.

A comparison was also made between theory and experiment at $\phi = 0.2$, as shown in Figs 9 and 10. As was seen for the 10% case, the simulations and the experiments at later times agree quite well. the peak in the initial RDF decreases indicating a decrease in the clustering and the curve shifts towards larger $x/\bar{R}_{PS}$ indicating a growth in the exclusion zone surrounding each of the particles. The change in both the experimental and theoretical PSDs over time is at most, very small, if at all. The experimentally determined RDF and PSD for the coarsening time of 14,400 s is shown in Figs 9(b) and 10(b). The agreement between the theoretical predictions and the experimental results are excellent at all coarsening times. Interestingly, the PSDs show little change even though the average particle size has increased by a factor of 2.3, while the change in the RDFs is readily apparent.

4. DISCUSSION

The evolution of the microstructure observed in the experiment can be modeled quite well using the transient AV simulations. Simulations clearly show how the clustered microstructure evolves towards the steady-state AV predictions. At 14,400 s, the longest coarsening time for which RDFs were measured, the microstructure with $\phi = 0.1$ had not yet reached steady-state. This transient evolution is

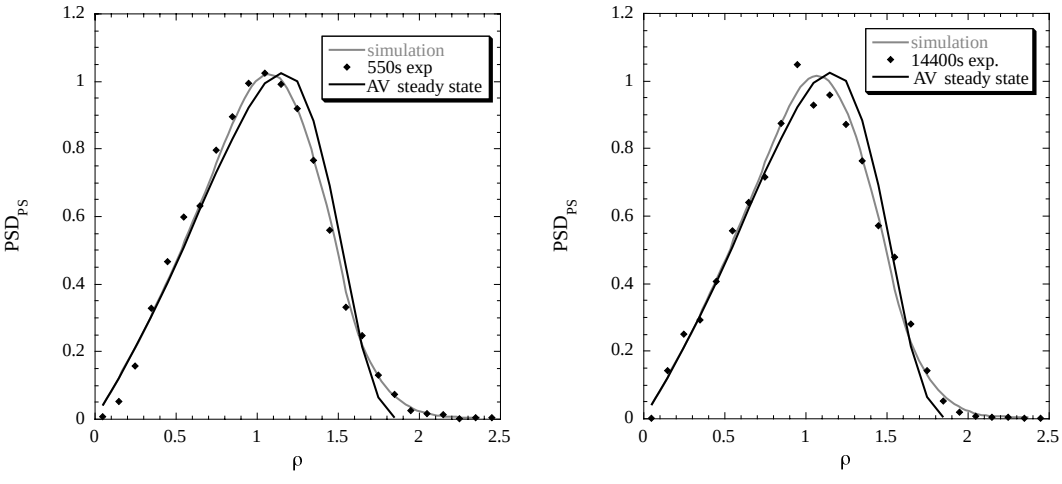

(a) $t = 550s$ (b) $t = 14400s$

Fig. 10. The evolution of the particle size distributions in the experiment and the simulations. The grey lines show results from the simulations, the diamonds show results from the experiment, and the black lines show the steady-state prediction at $\phi = 0.2$.

shown more clearly by the RDFs than the PSDs. This may not be the case, however, if the initial microstructure has a random spatial arrangement. From Fig. 5, we can estimate that the system with the initial experimental starting condition should reach steady-state after approximately 3×10^5 s, assuming $K_{LSW} = 1.6$ μm^3/s.

The simulations are extremely sensitive to initial conditions. Slight changes in the initial PSD and RDF can produce noticeable differences in the evolution of the microstructure. Although great care was taken in constructing the initial microstructures, small differences between the measured initial PSDs and RDFs and the simulation were unavoidable. This accounts for small differences in the PSDs, shown in Figs 8 and 10 and in [18].

An illustration of the sensitivity of the evolution of the PSD to the initial conditions is provided by Fig. 11. Here, the initial three-dimensional PSD used in the simulations is shown in Fig. 11(a) and the PSD corresponding to the longest experiment coarsening time in Fig. 11(b). The particles shown in Fig. 11(a) in the area shaded in grey, both light and dark, coarsen to particles in the corresponding shaded region in Fig. 11(b). The darker shaded region in Fig. 11(b) represents the approximate area where a slight difference between experiment and theory, shown in the plane section PSD in Fig. 8(d), occurs. The particles in this area can be traced back to particles in the darker shaded region in Fig. 11(a). This small area represents only 186 out of the original 50,000 particles used in the simulation. Thus, very small changes in the tail of the initial distribution have a large effect on the shape of the distribution at long periods of time. This directly illustrates the sensitivity of the simulations to the shape of the tail of the initial PSD and the difficulty in specifying the initial PSD with sufficient accuracy to produce good results at long coarsening times. This sensitivity, in the context of the LSW zero volume fraction theory of Ostwald ripening, has been emphasized recently by Niethammer and Pego [24].

Only plane section RDFs were measured. Ideally, the RDF should be measured in three dimensions, however, the large quantity of data required for such a measurement makes it difficult at this time. It would also be interesting to measure pair-correlation functions which develop during the experiment and compare these to theoretical findings. Again, this requires measurements in three dimensions.

We found that the clustered microstructure coarsened faster than the one with initially random correlations. This is expected since such a microstructure will have shorter diffusion distances and larger concentration gradients between particles within each cluster. Thus, these structures should ripen faster in the early stages of coarsening, until the clusters have evolved into isolated particles.

A few grain boundaries were present in the sample microstructures obtained from our experiments. During our image analysis procedure, particles connected by grain boundaries were separated so that particle sizes could be accurately measured. However, the number of boundaries present in the microstructure with $\phi = 0.1$ is so small that they should have a minimal affect. The magnitude of this effect at $\phi = 0.2$ is unclear. The effect of boundaries on the coarsening process is currently being investigated [25].

Using these simulations, we can determine a value of K_{LSW} similar to what was done in the previous AV simulations for the CSLM experiment [18]. We proceed by this method, since it appears that the experiments have not yet reached steady-state, where theoretical predictions for $f(\phi)$ are made. By comparing K_{LSW} determined using the simulations with that calculated from material parameters we can test the accuracy of the theory, even though the experiment might not have reached steady-state. We use the average radius measured as a function of time from the simulations and fit the data to the CSLM experiment results using K_{LSW} as the fit parameter. This can then be compared to the $K_{LSW} = 1.1 \pm 0.05$ μm^3/s† found by Hardy *et al.* in grain boundary groove experiments [23].

As reported previously [4], if we assume that the 10% volume fraction experiments have reached the steady-state regime, we can calculate a value of $K_{LSW} = 2.33$ μm^3/s based on the AV theory. The effect of transient coarsening is then included in the AV simulations by using the PSD measured for the experiment at 550 s and a random spatial distribution of particles. This reduces the value to $K_{LSW} = 1.9$ μm^3/s. The PSDs measured from coarsening experiments fit the theoretical transient predictions very well. The experimental distributions were not broader than the theoretical predictions, as was reported for many previous coarsening experiments. In the present work, we were also able to account for the effect of spatial correlations present in the initial system in the simulations. With these new simulations, we find $K_{LSW} = 1.6$ μm^3/s for $\phi = 0.1$ and $K_{LSW} = 1.7$ μm^3/s for $\phi = 0.2$. The fit between the experiment and theory is shown in Fig. 12. These two values for K_{LSW} are very close, indicating that the theory accounts for a change in K with ϕ quite well. Figures 7–10 also show that the experimentally measured RDFs and PSDs agree with those determined using the AV simulations. Accounting for both the initial PSD and RDF in

† The original value reported in the work by Hardy *et al.* was $K_{LSW} = 8/9A = 1.01 \pm 0.05$ μm^3/s. However, the fit in Fig. 13 of their paper was not done with equations (21) and (22), but instead allowed for a constant shift. By fixing this error, K_{LSW} becomes 1.1 μm^3/s.

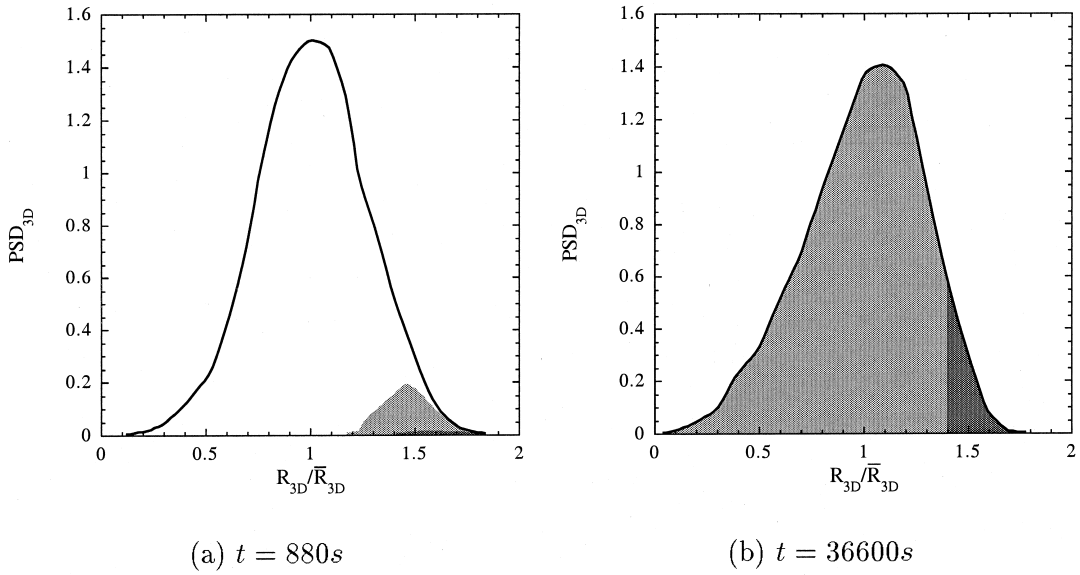

Fig. 11. (a) Initial and (b) final three-dimensional PSDs measured from the simulations. The area shaded in grey, both light and dark, represents the number of particles left in the simulations by the final coarsening time of 36,600 s. The particles in the dark grey area in (a) coarsen to those shown in the dark grey area in (b).

the transient simulations has brought us much closer to the value of K_{LSW} determined from grain boundary groove experiments. Such agreement leads us to believe that the AV theory is an excellent model for Ostwald ripening in ideal systems; other theories of Ostwald ripening remain to be tested. However, very few are formulated in a manner that permits them to be used to determine the evolution of a system in the transient regime. A far better alternative is to obtain data at longer coarsening times, when one would, in principle, be closer to steady state.

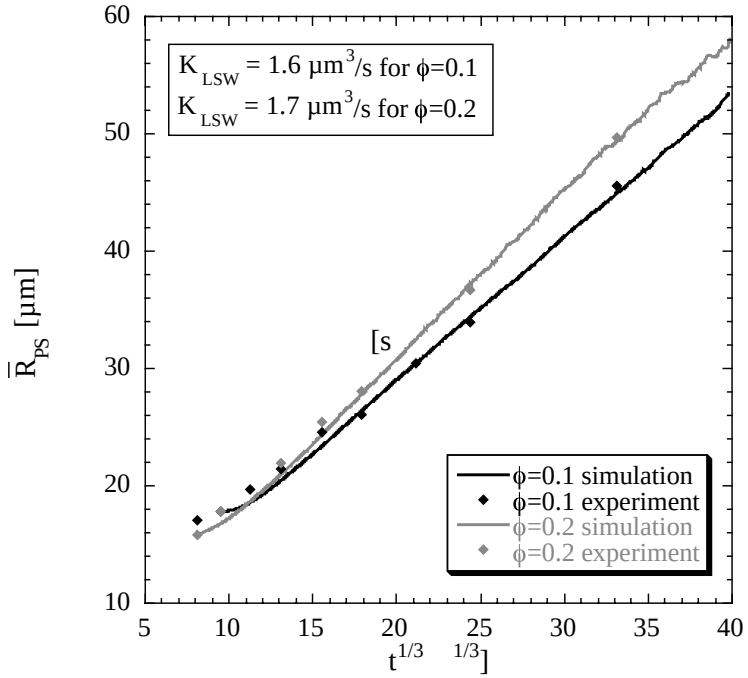

Fig. 12. AV simulation results were fit to the CSLM experiment results for $\phi = 0.1$ and $\phi = 0.2$ to determine K_{LSW}.

5. SUMMARY

Based on the results presented for the CSLM experiment and the simulations of transient Ostwald ripening we can draw a number of conclusions.

1. Plane section spatial correlation functions, measured in a low-volume fraction system undergoing Ostwald ripening, evolved towards, but never reached, the steady-state prediction. These correlations indicated that the microstructure initially consisted of clusters of particles and evolved into one which was more dispersed.
2. The initially highly correlated structure had no observable effect on the evolution of PSDs, but did have an effect on the coarsening rate of the system.
3. The spatial correlation functions measured from the experiment were a much more sensitive measure of the presence of steady-state coarsening than the PSDs.
4. A structure consisting of clusters of particles coarsened faster than a system with a random, non-overlapping spatial arrangement.
5. The spatial correlation functions and the PSDs measured from the experiment agreed well with those calculated from the AV simulations using the initial experimental correlations and PSD. The value of K_{LSW} that was determined from these simulations was also close to the value measured in grain boundary groove experiments and approximately constant for volume fractions of 0.1 and 0.2 coarsening phase. Thus, we find that the AV simulations are an excellent model for coarsening in ideal systems.

Acknowledgements—The financial support of the Microgravity Sciences Research Division of NASA and a National Science Foundation Graduate Fellowship (V.S.) are gratefully acknowledged. We would also like to thank Norio Akaiwa for making his simulation program available for this study.

REFERENCES

1. Lifshitz, I. M. and Slyozov, V. V., *J. Phys. Chem. Solids*, 1961, **19**, 35.
2. Wagner, C., *Z. Elektrochem.*, 1961, **65**, 581.
3. Hardy, S. C. and Voorhees, P. W., *Metall. Mater. Trans.*, 1988, **19A**, 2713.
4. Akaiwa, N. and Voorhees, P., *Phys. Rev. E*, 1994, **49**(5), 3860.
5. Voorhees, P. W. and Glicksman, M. E., *Acta metall.*, 1984, **32**(11), 2001.
6. Voorhees, P. W. and Glicksman, M. E., *Acta metall.*, 1984, **32**(11), 2013.
7. Marqusee, J. A. and Ross, J., *J. chem. Phys.*, 1984, **80**(1), 536.
8. Brailsford, A. D. and Wynblatt, P., *Acta metall.*, 1979, **27**, 489.
9. Marsh, S. P. and Glicksman, M. E., TMS, Warrendale, 1992.
10. Beenakker, C. W. J., *Phys. Rev. A*, 1986, **33**(6), 4482.
11. Tokuyama, M. and Kawasaki, K., *Physica A*, 1984, **123**, 386.
12. Marder, M., *Phys. Rev. Lett.*, 1985, **55**(27), 2953.
13. Ardell, A. J., *Acta metall.*, 1972, **20**.
14. Akaiwa, N. and Meiron, D. I., *Phys. Rev. E*, 1995, **51**(6), 5408.
15. Krichevsky, O. and Stavans, J., *Phys. Rev. Lett.*, 1993, **70**(10), 1473.
16. Seyhan, I., Ratke, L., Bender, W. and Voorhees, P. W., *Metall. Mater. Trans.*, 1996, **27A**, 2470.
17. Bender, W. and Ratke, L., *Acta metall.*, 1998, **46**, 1125.
18. Alkemper, J., Snyder, V., Akaiwa, N. and Voorhees, P. W., *Phys. Rev. Lett.*, 1999, **82**(13), 2725.
19. Abis, S., *et al.*, *Mat. Sci. Engng*, 1995, **32B**, 169.
20. Gokhale, A. M., In *NASA Microgravity Materials Science Conference*, 1996.
21. White, W. R. and Wiltzius, P., *Phys. Rev. Lett.*, 1995, **75**(16), 3012.
22. Chen, M. K. and Voorhees, P. W., *Modelling Simul. Mater. Sci. Engng*, 1993, **1**, 591.
23. Hardy, S. C., McFadden, G. B., Coriell, S. R., Voorhees, P. W. and Sekerka, R. F., *J. Cryst. Growth*, 1991, **114**, 467.
24. Niethammer, B. and Pego, R., Preprint, 1999.
25. Eggleston, J., Snyder, V. A., Alkemper, J. and Voorhees, P. W., Unpublished research, 2000.